Inorg. Chem. **2005**, *44*, 6197−6202

Synthesis, Structure, and Magnetic Properties of the Oxalate-Based Bimetallic Ferromagnetic Chain $\{[K(18\text{-crown-6})][Mn(H_2O)_2Cr(ox)_3]\}_\infty$ (18-crown-6 = $C_{12}H_{24}O_6$, ox = $C_2O_4^{2-}$)

Eugenio Coronado,* José R. Galán-Mascarós,* Carlos J. Gómez-García, and Carlos Martí-Gastaldo

Instituto de Ciencia Molecular, Universidad de Valencia, C/Doctor Moliner 50, 46100 Burjassot, Spain

Received February 18, 2005

The salt $[K(18\text{-crown-6})][Mn(H_2O)_2Cr(ox)_3]\cdot 0.5(18\text{-crown-6})$ (**1**) has been prepared and structurally and magnetically characterized. It crystallizes in the $P2_1/c$ space group [a = 21.011(2) Å, b = 11.265(2) Å, c = 15.748(3) Å, β = 105.952(6)°, V = 3584(1) Å^3, and Z = 4] and contains $[Mn(H_2O)_2Cr(ox)_3]_\infty$ chains connected through hydrogen bonding to form 2D anionic networks. The magnetic exchange is ferromagnetic [J = +2.23(2) cm^{-1}] in the chain and also in between chains, reaching bulk ferromagnetic ordering below 3.5 K.

Introduction

Oxalate bimetallic complexes have been used extensively for the construction of magnetic materials since the discovery, more than 10 years ago, of ferro- and ferrimagnetism in the bimetallic layered oxalate-bridged compounds of the general formula $A[M^{II}M^{III}(ox)_3]$.[1] In this approach, the octahedral tris(oxalato)metal complexes of trivalent metals were used as ligands toward paramagnetic divalent metal ions to build 2D honeycomb hexagonal networks.[2] The driving force in the preparation of these compounds is related to the use of bulky templating cations able to stabilize the formation of such anionic layers, for example, tetraalkylammonium derivatives. The oxalate ligand is responsible for promoting strong enough magnetic superexchange to give rise to magnetic ordering with critical temperatures between 6 and 45 K.[3,4] Taking advantage of the layered nature of these oxalate-based magnets, multifunctional magnetic materials have been prepared using electroactive cations in the role of the tetraalkylammonium derivatives. Magnetic multilayers,[5] photoactive magnets,[6] and the first family of molecular ferromagnetic metals[7,8] are the most interesting results in this context.

From the point of view of molecule-based magnetic materials, oligomeric species have been successfully prepared following this bimetallic approach but limiting the growth of the bimetallic complexes. With the help of capping ligands, oxalate-bridged dimers,[9] trimers,[10] or tetramers[11]

* To whom correspondence should be addressed. E-mail: eugenio.coronado@uv.es (E.C.), jose.r.galan@uv.es (J.R.G.-M.).

(1) Tamaki, H.; Zhong, Z. J.; Matsumoto, N.; Kida, S.; Koikawa, M.; Achiwa, N.; Hashimoto, Y.; Okawa, H. *J. Am. Chem. Soc.* **1992**, *114*, 6974−6979.
(2) Pellaux, R.; Schmalle, H. W.; Huber, R.; Fisher, P.; Hauss, T.; Ouladdiaf, B.; Decurtins, S. *Inorg. Chem.* **1997**, *36*, 2301−2308.
(3) (a) Tamaki, H.; Mitsumi, M.; Nakamura, N.; Matsumoto, N.; Kida, S.; Okawa, H.; Ijima, S. *Chem. Lett.* **1992**, 1975−1978. (b) Okawa, H.; Matsumoto, N.; Tamaki, H.; Ohba, M. *Mol. Cryst. Liq. Cryst.* **1993**, *232*, 617−622.
(4) (a) Mathonière, C.; Carling, S. G.; Yusheng, D.; Day, P. *J. Chem. Soc., Chem. Commun.* **1994**, 1551−1552. (b) Mathonière, C.; Nutall, J.; Carling, S. G.; Day, P. *Inorg. Chem.* **1996**, *35*, 1201−1206.
(5) (a) Coronado, E.; Galán-Mascarós, J. R.; Gómez-García, C. J.; Ensling, J.; Gütlich, P. *Chem.—Eur. J.* **2000**, *6*, 552−563. (b) Coronado, E.; Galán-Mascarós, J. R.; Gómez-García, C. J.; Martínez-Agudo, J. M. *Adv. Mater.* **1999**, *11*, 558−561. (c) Clemente-León, M.; Coronado, E.; Galán-Mascarós, J. R.; Gómez-García, C. J. *Chem. Commun.* **1997**, 1727−1728.
(6) (a) Bénard, S.; Yu, P.; Audière, J. P.; Rivière, E.; Clèment, R.; Ghilhem, J.; Tchertanov, L.; Nakatani, K. *J. Am. Chem. Soc.* **2000**, *122*, 9444−9454. (b) Bénard, S.; Rivière, E.; Yu, P.; Nakatani, K.; Delouis, J. F. *Chem. Mater.* **2001**, *13*, 159−162.
(7) Coronado, E.; Galán-Mascarós, J. R.; Gómez-García, C. J.; Laukhin, V. *Nature* **2000**, *408*, 447−449.
(8) (a) Alberola, A.; Coronado, E.; Galán-Mascarós, J. R.; Giménez-Saiz, C.; Gómez-García, C. J. *J. Am. Chem. Soc.* **2003**, *125*, 10774−10775. (b) Alberola, A.; Coronado, E.; Galán-Mascarós, J. R.; Giménez-Saiz, C.; Gómez-García, C. J.; Romero, F. M. *Synth. Met.* **2003**, *133*−*134*, 509−513. (c) Alberola, A.; Coronado, E.; Galán-Mascarós, J. R.; Giménez-Saiz, C.; Gómez-García, C. J.; Martínez-Ferrero, E.; Murcia-Martínez, A. *Synth. Met.* **2003**, *135*−*136*, 687−689.
(9) Triki, S.; Berezovsky, F.; Pala, J. S.; Coronado, E.; Gómez-García, C. J.; Clemente, J. M.; Riou, A.; Molinie, P. *Inorg. Chem.* **2000**, *39*, 3771−3776.
(10) (a) Rochon, F. D.; Melanson, R.; Andruh, M. *Inorg. Chem.* **1996**, *35*, 6086−6092. (b) Andruh, M.; Melanson, R.; Stager, C. V.; Rochon, F. D. *Inorg. Chim. Acta* **1996**, 309−317. (c) Stanica, N.; Stager, C. V.; Cimpoesu, M.; Andruh, M. *Polyhedron* **1998**, *17*, 1787−1789.
(11) (a) Coronado, E.; Giménez, M. C.; Gómez-García, C. J.; Romero, F. M. *Polyhedron* **2003**, *22*, 3115−3122. (b) Marinescu, G.; Andruh, M.; Lescouëzec, R.; Muñoz, M. C.; Cano, J.; Lloret, F.; Julve, M. *New J. Chem.* **2000**, *24*, 527−536.

10.1021/ic050258w CCC: $30.25
Published on Web 08/02/2005

have been obtained. Also pure oxalate complexes as dimers[12] or trimers[13] have been isolated by controlling the synthesis and solubility of the species in the reaction media.

In the opposite direction, the dimensionality could also be increased, yielding the preparation of 3D bimetallic networks of the general formula $[Z(bpy)_3][ClO_4][M^{II}M^{III}(ox)_3]$ ($Z = Fe^{II}$, Co^{II}, Ni^{II}, Ru^{II}),[14] where the tris-bipyridyl complexes are the templating cations for the stabilization of the decagon extended network, with the extra perchlorate anion occupying holes left in the structure for electroneutrality. The peculiarity of these systems resides in the homochirality of all of their metal centers, while in their 2D counterparts, the adjacent metal centers exhibit alternated chirality. These homochiral polymers are not planar because geometrically it is not possible to stay in the plane with only one diastereoisomer as the building block. These 3D analogues behave also as ferro- and ferrimagnets but with lower ordering temperatures. This indicates weaker magnetic exchange due to the different relative orientation of the magnetic orbitals and also to the longer metal to metal distances, while the magnetic connectivity is identical despite the higher structural dimensionality.

As described before, the shape, size, geometry, and charge of the cations are key elements for the preparation of the different oxalate-based architectures. With this in mind, we tried to use the $[K(18\text{-crown-6 ether})]^+$ cation because its planar shape and bulkiness could induce novel structural motifs. As a result, here we report on the synthesis, structure, and magnetic properties of the 1D oxalate-bridged bimetallic chain $[K(18\text{-crown-6})][Mn(H_2O)_2Cr(ox)_3]\cdot 0.5(18\text{-crown-6})$ (**1**).

Experimental Section

Synthesis. All reagents and solvents used were of commercially available grade. $K_3[Cr(ox)_3]$ was prepared following the literature procedure.[15] $[K(18\text{-crown-6})][Mn(H_2O)_2Cr(ox)_3]\cdot 0.5(18\text{-crown-6})$ (**1**) was obtained by slow difussion of a methanolic solution (15 mL) of $K_3[Cr(ox)_3]$ (0.487 g, 1 mmol) with excess 18-crown-6 ether (1.320 g, 5 mmol) into a water solution (10 mL) of $MnCl_2\cdot 4H_2O$ (0.198 g, 1 mmol). Long prismatic crystals of **1** were obtained in the interphase after several days, filtered out, and dried in air at room temperature. For X-ray crystal diffraction, the crystals were rapidly cooled to 180 K because when still wet, the water present in the mother liquor partially dissolves them as methanol evaporates faster at room temperature. Yield: 0.21 g (25%). Anal. Calcd for $C_{24}H_{40}CrKMnO_{23}$: C, 33.50; H, 4.92. Found: N, 0.09; C, 33.49; H, 4.95. IR (KBr): ν_{as}(O−C−O) 1686, 1655, 1640, 1627 cm^{-1}.

X-ray Crystallography. A dark purple prismatic single crystal of **1** ($0.3 \times 0.2 \times 0.2$ mm) was fixed on a glass fiber and mounted on a Kappa CCD diffractometer equipped with graphite-monochromated Mo Kα radiation ($\lambda = 0.710\,73$ Å). Cell refinements and data reduction were performed at 180 K using the Denzo and Scalepack programs.[16] The structure was solved by direct methods using the SIR97 program[17] and refined on F^2 with the SHELXL-97 program.[18] The 18-crown-6 ether ring around the K position appears disordered over two possible configurations, rotated 15° with respect to one another and each refined with 50% occupancy. H atoms from the water molecules bound to the Mn atoms were found after successive Fourier differences and refined, maintaining all O−H distances equal. The positions for the rest of the H atoms were calculated, and all thermal parameters for the H atoms were fixed to be 50% larger than those of the atoms to which they are bound. All non-hydrogen atoms were refined anisotropically, except those corresponding to the disordered 18-crown-6 ether rings. Crystal, data collection, and refinement parameters are summarized in Table 1.

Table 1. Main Structural Parameters and Crystallographic Data for the Salt **1**[a]

formula	$C_{24}H_{40}CrKMnO_{23}$
M_w	842.60
space group	$P2_1/c$
a (Å)	21.011(2)
b (Å)	11.265(2)
c (Å)	15.748(3)
β (deg)	105.952(6)
V (Å^3)	3584(1)
Z	4
T (K)	180(2)
λ (Å)	0.71073
ρ_{calc} (g/cm^3)	1.562
μ (mm^{-1})	0.859
R1	0.0549
wR2	0.1174

[a] $R1 = \sum(F_o - F_c)/\sum(F_o)$. $wR2 = [\sum[w(F_o^2 - F_c^2)^2]/\sum[w(F_o^2)^2]]^{1/2}$; $w = 1/[\sigma^2(F_o^2) + (0.0443P)^2 + 7.5713P]$ where $P = (F_o^2 + 2F_c^2)/3$.

CCDC-258980 contains the supplementary crystallographic data for this paper. It can be obtained free of charge via www.ccdc.cam.ac.uk/retrieving.html (or from the Cambridge Crystallographic Data Centre, 12 Union Road, Cambridge CB2 1EZ, U.K., deposit@ccdc.cam.ac.uk).

Before and after the magnetic measurements, X-ray powder profiles of the sample were collected (Figure S1 in the Supporting Information) using a Siemens D-500 X-ray diffractometer (Cu Kα radiation, $\lambda_\alpha = 1.541\,84$ Å). Samples were grounded and mounted on a flat sample plate. Typically, profiles were collected as step scans over a 12-h period in the $2° < 2\theta < 60°$ range with a step size of 0.02°. All patterns were analogous and in good agreement with the theoretical X-ray powder pattern simulated with the atomic positions obtained from the single-crystal data, which confirms that the compound does not overcome any structural transition when dried.

Physical Measurements. Magnetic measurements were carried out with a Quantum Design (SQUID) magnetometer MPMS-XL-5. DC measurements were performed with an applied field of 100 G (10^{-2} T) in the 2−300 K temperature range. AC measurements were performed with an alternating field of 3.95 G (3.95×10^{-4} T) at different frequencies between 1 and 1000 Hz. Data were

(12) (a) Coronado, E.; Galán-Mascarós, J. R.; Gómez-García, C. J. *Dalton Trans.* **2000**, 205−210. (b) Rashid, S.; Turner, S. S.; Day, P.; Light, M. E.; Hursthouse, M. B. *Inorg. Chem.* **2000**, *39*, 2426−2428.
(13) (a) Coronado, E.; Galán-Macarós, J. R.; Giménez-Saiz, C.; Gómez-García, C. J.; Ruiz-Pérez, C. *Eur. J. Inorg. Chem.* **2003**, 2290−2298. (b) Coronado, E.; Galán-Mascarós, J. R.; Giménez-Saiz, C.; Gómez-García, C.; Ruiz-Pérez, C.; Triki, S. *Adv. Mater.* **1996**, *8*, 737−740.
(14) Coronado, E.; Galán-Mascarós, J. R.; Gómez-García, C. J.; Martínez-Agudo, J. M. *Inorg. Chem.* **2001**, *40*, 113−120.
(15) Baylar, J. M.; Jones, E. M. In *Inorganic Synthesis*; Booth, H. S., Ed.; McGraw-Hill: New York, 1939.
(16) Otwinowski, Z.; Minor, W. In *Methods in Enzymology*; Carter, C. W., Jr., Sweet, R. M., Eds.; Academic Press: New York, 1997; Vol. 276, pp 307−326.
(17) SIR97: Altomare, A.; Burla, M. C.; Camali, M.; Cascarano, G. L.; Giacovazzo, C.; Guagliardi, A.; Moliterni, A. G. G.; Polidori, G.; Spagna, R. *J. Appl. Crystallogr.* **1999**, *32*, 115−119.
(18) Sheldrick, G. M. SHELXL-97, University of Göttingen, Göttingen, Germany, 1997.

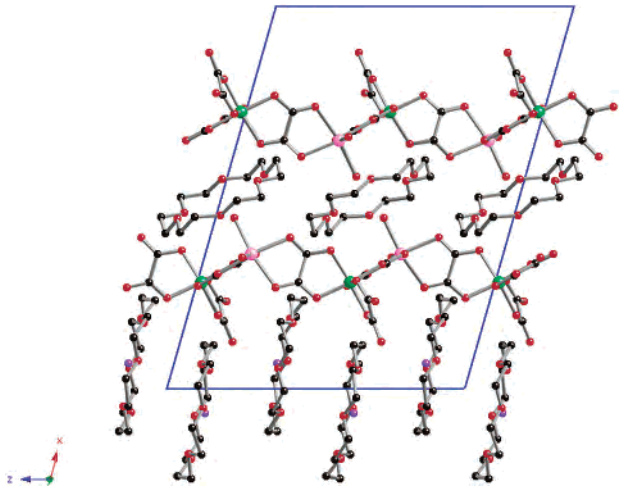

Figure 1. Projection on the *ac* plane of the crystal structure of **1** showing the alternating layers along the *a* axis.

corrected for the diamagnetic contributions calculated using the Pascal constants. Calorimetric measurements were performed on pressed pellets with a Quantum Design PPMS in the 2−20 K range.

Synthesis and Crystal Structure

Slow diffusion of a methanolic solution of $K_3[Cr(ox)_3]$ with an excess of 18-crown-6 ether into a water solution containing $[Mn(H_2O)_6]^{2+}$ cations yields chunky crystals of **1** after several days. **1** is soluble in water but insoluble in methanol or other organic solvents. Although obtained by slow diffusion, it seems to be a kinetic product. Actually, the analogous bulk reaction yields insoluble products different from the title compound that have to be characterized yet, and **1** is not even obtained if the slow diffusion is done at temperatures slightly higher than room temperature (over 30 °C). Therefore, the preparation and isolation of **1** requires very specific synthetic conditions, and a careful procedure, because other products may be present. For all characterizations, single crystals were hand collected to ensure that no other phase was present, and the unit cell of crystals of every batch prepared was checked by single-crystal and powder X-ray diffraction.

The structure of **1** is built from three different types of segregated layers, formed respectively by [K(18-crown-6 ether)]$^+$ units (A), $[Mn(H_2O)_2Cr(ox)_3]^-$ complexes (B), and neutral 18-crown-6 ether molecules (C), alternating along the *a* axis (Figure 1), with a repeating pattern ...BCBA .... The anionic layers contain 1-D chains formed by alternating $[Cr(ox)_3]^{3-}$ and Mn^{2+} ions bridged by oxalate units (Figure 2). The Cr centers maintain the regular octahedral geometry, even when one of the oxalate ligands is terminal, with all Cr−O distances in a 0.05-Å range. The small distortion comes from the bite angle of the oxalate ligands, which deviates slightly from that of the regular octahedral [O−Cr−O = 83(1)°]. The Mn centers, chelated by two oxalate ligands, complete their octahedral coordination sphere with two water molecules in the cis conformation. Thus, they are slightly more distorted, with Mn−O_w distances (≈2.14 Å) shorter than the corresponding Mn−O_{ox} (2.173 Å < Mn−O < 2.261 Å) and a more acute bite angle imposed by the oxalate ligands [O−Mn−O = 76(1)°].

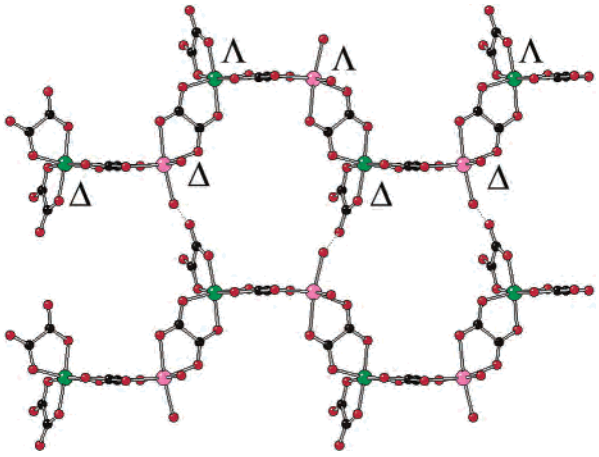

Figure 2. View of the $\{[Mn(H_2O)_2Cr(ox)_3]\}_n^{n-}$ chains showing the hydrogen-bonded network in the anionic layers in **1**.

The chains are formed by both possible enantiomers present by pairs, with a repeating unit −ΔΔΛΛ−, in such a way that each Cr^{III} ion is connected to two Mn^{II} centers, one Δ and one Λ, and vice versa, creating a zigzag shape (Figure 2). One water molecule bound to the Mn ions points toward the neutral 18-crown-6 ether layer, while the other water molecule bound to the Mn ions remain in the plane of the layers, forming a quite strong hydrogen bond (O···O = 2.176 Å) with an oxygen atom from a terminal oxalate group from a neighboring chain. In this way, all chains perfectly match on the plane, creating a shape reminiscent of typical honeycomb networks. It needs to be pointed out that these chains cannot be regarded as intermediate building blocks for a possible honeycomb network because for such a structure strictly alternation of chiral centers is needed, which does not happen in these chains. The other oxygen atom from the terminal oxalate group points toward the cationic layers and weakly interacts with a K^+ atom (O···K = 2.654 Å). This interaction makes the K^+ atoms be slightly above the mean plane determined by the O atoms of the crown ether ligand [0.35(2) Å]. This interaction also dictates the packing of the cationic complexes in the layer, which appear perpendicular to the plane and arranged in dimers following a pseudohexagonal pattern. The crown ether molecules appear disordered over two crystallographic positions, rotated 15° with respect to one another, with both being equivalent from the point of view of bonding distances to the central K atom.

Each neutral layer is sandwiched by two anionic layers in such a way that oxygen atoms from the 18-crown-6 ether molecules, which lack any ion in their cavities, show some H-bonding contacts (O···O = 2.778 and 2.879 Å) with two water molecules from the adjacent anionic layers, one above and one below, that also come close between them (Ow···Ow = 2.931 Å). These weak hydrogen-bonding interactions in the solid state impose these crown ether molecules to appear perfectly ordered, in contrast to the ones belonging to the cationic layer.

The metal−metal distances in the chain (5.433 Å) are shorter than those between chains (7.415 Å); thus, the magnetic interacions should be weaker, although not negli-

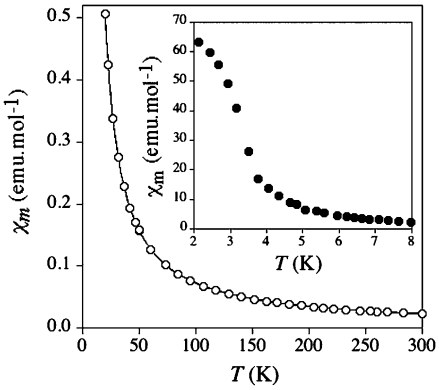

Figure 3. Thermal dependence of the DC magnetic susceptibility for **1** with the best fitting of the high-temperature data to a 1D chain bimetallic model.

gible. In addition, the strong hydrogen bonding between the oxalate bound to a Cr and the water molecule bound to a Mn could also have an important role in this regard, as will be discussed later.

Magnetic Properties

The magnetic measurements were performed on grounded single crystals between 2 and 300 K. $\chi_m T$ (Figure S2 in the Supporting Information) remains almost constant when cooling the sample from room temperature, with a small positive slope, until below 20 K, when it begins to increase very rapidly, going over 150 emu K mol^{-1} below 3 K. This fast increase corresponds to a jump that is observed in the χ vs T plot (Figure 3), with the magnetic susceptibility reaching saturation below 3 K. These features clearly suggest the onset of magnetic ordering. The 50−300 K data can be fitted to a Curie−Weiss law (see the Supporting Information) with $C = 6.62$ emu K mol^{-1} ($\bar{g} \approx 2.06$) in good agreement with the expected spin-only value of 6.25 emu K mol^{-1} and a positive $\theta = +8.1$ K, indicating the presence of ferromagnetic coupling between Cr^{III} and Mn^{II}. The data can also be fitted in the paramagnetic range, well above the onset of the long-range magnetic ordering (10−300 K) to the equation developed for a Heisenberg 1D chain with alternating spins,[19] from the Hamiltonian

$$H = -\sum_{i=0}^{N} J S_i S_{i+1} \qquad (1)$$

$$\chi_m = \frac{N_A \mu_B^2}{6kT}\left[M^2\frac{1+P}{1-P} + (\delta M)^2\frac{1-P}{1+P}\right]$$

where $P = \coth(J_{eff}/kT) - (kT/J_{eff})$, $M = M_{Mn} + M_{Cr}$, $\delta M = M_{Mn} - M_{Cr}$, $M_i = g_i\sqrt{S_i(S_i+1)}$, and $J_{eff} = J\sqrt{S_{Mn}(S_{Mn}+1)S_{Cr}(S_{Cr}+1)}$ as the magnetic interactions between metal centers. A mean g value for both ions was used for the model. The fitting is very satisfactory, giving $\bar{g} = 2.094(2)$ and $J = +2.23(2)$ cm^{-1}, with the same sign and order of magnitude as those found in other oxalate-bridged Mn−Cr complexes.[13] As seen in all previous works, the interaction between Cr^{III} and Mn^{II} through an oxalate bridge in its chelating form is expected to be ferromagnetic, and that is obviously the case for this new chain, as confirmed by the positive value of J (and of θ).

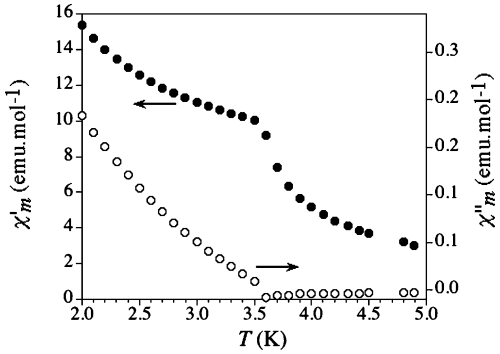

Figure 4. Thermal dependence of the AC magnetic susceptibility for **1**.

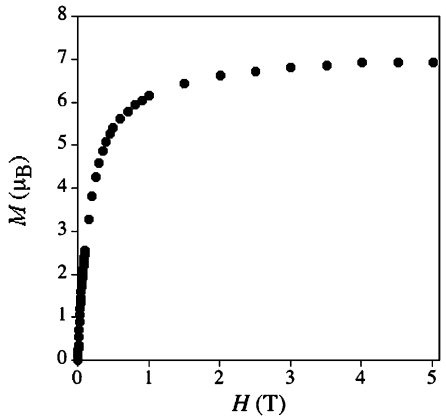

Figure 5. Field dependence of the magnetization at 2 K for **1**.

The AC magnetic susceptibility measurements (Figure 4) confirm the onset of magnetic ordering, showing a peak in the in-phase signal (χ'_m) and a nonzero out-of-phase signal (χ''_m), below 3.5 K, defining T_c. These measurements are not frequency-dependent, with the behavior of the susceptibilities remaining the same in all frequencies explored (between 1 and 1000 Hz). χ''_m, instead of a typical peak expected for a classic 3D ferromagnet, increases continuously down to 2 K, with a slight change in the slope at 2.7 K, suggesting the presence of at least two contributing processes, both of them frequency-independent. This complex ac susceptibility behavior has already been seen in other low-dimensional molecule-based magnets.[20]

The ferromagnetic nature of the magnetic ordering in this material is confirmed by the field dependence of the magnetization (Figure 5). At 2 K, it shows a very rapid increase for small fields, reaching a saturation value of 6.92 μ_B at 5 T. This value is slightly lower than that expected for a parallel alignment of the two interacting spins (8 μ_B) but in good agreement with those found in the family of oxalate-bridged bimetallic structures,[1,5] the reason being the spin canting present in the ferromagnetic state. The hysteresis loop

(19) Mosset, A.; Galy, J.; Coronado, E.; Drillon, M.; Beltran, D. *J. Am. Chem. Soc.* **1984**, *106*, 2864−2869.

(20) (a) Bellouard, F.; Clemente-León, M.; Coronado, E.; Galán-Mascarós, J. R.; Gómez-García, C. J.; Romero, F. M.; Dunbar, K. R. *Eur. J. Inorg. Chem.* **2002**, 1603−1606. (b) Thétiot, F.; Triki, S.; Sala-Pala, J.; Gómez-García, C. J.; Golhen, S. *Chem. Commun.* **2002**, 1078−1079.

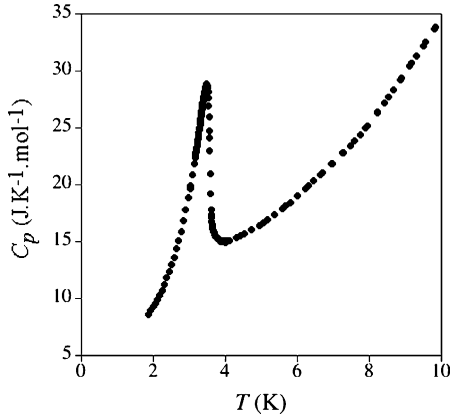

Figure 6. Calorimetric measurements for **1**.

shows no measurable coercive field; therefore, this material behaves as a soft ferromagnet.

The ferromagnetic ordering must be the result of interchain interactions of positive sign. As indicated by the high-temperature behavior of the magnetic moment, the intrachain interactions are ferromagnetic, but also ferromagnetic interactions between chains must be present for the overall ferromagnetic ordering observed, induced by dipolar interactions and also by a possible superexchange pathway that can work through the hydrogen bonding present between chains in the layer. Both mechanisms yield rather weak magnetic exchange but strong enough to promote the onset of ferromagnetic ordering, taking into account that even when the coupling is small, it occurs between large spins in the corresponding ferromagnetic chains. The interaction between the layers should be weaker, and therefore the system could be considered quasi-2D. It is important to note that this structure is reminiscent of the well-known 2D honeycomb magnets,[2] with the important difference being the substitution of a oxalate bridge by a water−oxalate hydrogen bonding. This is clearly one of the reasons why the critical temperature for the magnetic ordering is 3 K below that found for the honeycomb 2D analogue, which is around 6 K.

To confirm the appearance of magnetic ordering, we performed specific heat capacity measurements in the range of 2−20 K (Figure 6). The plot shows how the temperature dependence deviates from the lattice-only background and shows a typical λ peak with a maximum at 3.5 K. This feature confirms the presence of magnetic ordering at this critical temperature.

Conclusion

We have prepared and structurally characterized the first bimetallic oxalate-bridged ferromagnetic chain $[Mn(H_2O)_2Cr(ox)_3]_n^{n-}$ using as a template the cation $[K(18\text{-crown-6})]^+$, in the presence of excess of 18-crown-6 ether. This chain is soluble in polar solvents, and it can only be isolated under particular synthetic conditions as an insoluble product. It is also important to note that it is formed from both enantiomers of the corresponding octahedral metallic complexes, but instead of following a typical alternating arrangement, the complexes appear as pairs of identical chirality (−ΔΔΛΛ−). In the solid state, these chains are connected to each other through strong hydrogen bonding in 2D, and also weakly in 3D, which clearly affects the magnetic properties. In fact, ferromagnetic ordering is observed below 3.5 K, arising from the ferromagnetic intrachain interactions and from weak ferromagnetic interchain interactions through the hydrogen-bonded pathway, which happens to be also of ferromagnetic nature. The participation of hydrogen bonding in the overall magnetic superexchange makes this material show a lower critical temperature when compared with the analogous well-known 2D honeycomb bimetallic layers.

It is important to note that, although many bimetallic chain compounds are known in molecule-based magnetic materials, most of them are commonly ferrimagnetic chains,[21] and few ferromagnetic chains have been characterized.[22] In both cases, antiferromagnetic interactions between chains are usually found, giving rise to antiferromagnetic ordering[23] and to metamagnetic behavior in some cases.[24] In general, few examples of ferromagnets based in 1D systems have been reported to date.[25] Related to oxalate complexes in particular, there is only one other example of a bimetallic chain. This chain adopts a ladderlike structure built from bis(bidentate)-bridged $[Mn(H_2O)_2Cr(ox)_3]^-$ dimers bound through a monodentate/bidentate oxalate bridge along the axis of the chain. The two different bridging modes between the metal centers promote the coexistence of ferro- and antiferromagnetic interactions.[26]

This synthetic approach can now be extended to other metals to tune the magnetic properties. For instance, the use of $[Fe(ox)_3]^{3-}$ instead of $[Cr(ox)_3]^{3-}$ while maintaining the same structure should favor stronger magnetic interactions of the opposite sign (AF), which would promote higher critical temperatures, such as those observed in the 2D or 3D magnets. Substitution of Mn^{II} by other divalent cations such as Fe^{II}, Co^{II}, or Ni^{II} should also have interesting effects on the magnetic properties.

We are also studying in detail the synthetic conditions that yielded this compound because this chain proves that isolation of products with unusual structural features and properties can be obtained from the building blocks for polymeric oxalate-based magnets. Preliminary results indicate that other intermediate phases between dimensionalities zero and two can also be obtained.

Finally, regarding the recent interest in chain compounds due to the discovery of the so-called "single-chain magnets",[27] we are also exploring the use of organic chelating

(21) (a) Kahn, O. *Acc. Chem. Res.* **2000**, *33*, 647−657. (b) Gleizes, A.; Verdaguer, M. *J. Am. Chem. Soc.* **1984**, *106*, 3727−3737.
(22) (a) Ohba, M.; Usuki, N.; Fukita, N.; Okawa, H. *Inorg. Chem.* **1998**, *37*, 3349−3354. (b) Ohba, M.; Maruono, N.; Okawa, H.; Enoki, T.; Latour, J.-M. *J. Am. Chem. Soc.* **1994**, *116*, 11566−11567.
(23) Coronado, E.; Drillon, M.; Nugteren, P. R.; De Jongh, L. J.; Beltran, D.; Georges, R. *J. Am. Chem. Soc.* **1989**, *111*, 3874−3880.
(24) (a) Colacio, E.; Ghazi, M.; Stoeckli-Evans, H.; Lloret, F.; Moreno, J. M.; Perez, C. *Inorg. Chem.* **2001**, *40*, 4876−4883. (b) Kahn, O.; Bakalbasis, E.; Mathoniere, C.; Hagiwara, M.; Katsumata, K.; Ouahab, L. *Inorg. Chem.* **1997**, 15300−1531.
(25) (a) Re, N.; Floriani, C.; Miyasaka, H.; Matsumoto, N. *Inorg. Chem.* **1996**, *35*, 6004−6008. (b) Miller, J. S.; Calabrese, J. C.; Rommelmann, H. R.; Chittipeddi, S. R.; Zhang, J. H.; Reiff, W. M.; Epstein, A. J. *J. Am. Chem. Soc.* **1987**,
(26) Alberola, A.; Coronado, E.; Giménez-Saiz, C.; Gómez-García, C. J.; Romero, F. M.; Tarazón, A. *Eur. J. Inorg. Chem.* **2005**, 389−400.

ligands able to substitute the water molecules binding the M^{II} centers. This will break the H bonding and enlarge the interchain distances; required features if oxalate-based chains may also give rise to such unusual magnetic behavior.

(27) (a) Caneschi, A.; Gatteschi, D.; Lalioti, N.; Sangregorio, C.; Sessoli, R.; Venturi, G.; Vindigni, A.; Rettori, A.; Pini, M. G.; Novak, M. A. *Angew. Chem., Int. Ed.* **2001**, *40*, 1760−1763. (b) Clerac, R.; Miyasaka, H.; Yamashita, M.; Coulon, C. *J. Am. Chem. Soc.* **2002**, *124*, 12837−12844. (c) Lescouezec, R.; Vaissermann, J.; Ruiz-Perez, C.; Lloret, F.; Carrasco, R.; Julve, M.; Verdaguer, M.; Dromzee, Y.; Gatteschi, D.; Wernsdorfer, W. *Angew. Chem., Int. Ed.* **2003**, *42*, 1483−1486.

Acknowledgment. This work was supported by the Ministerio de Educación y Ciencia (Projects MAT2004-3849 and BQU2002-01091). C.M.G. thanks the Ministerio de Educación y Ciencia for a predoctoral fellowship.

Supporting Information Available: CIF data and figures of experimental and theoretical powder patterns and plot of $\chi_m T$ vs T for compound **1**. This material is available free of charge via the Internet at http://pubs.acs.org.

IC050258W